

Acetone sensors for non-invasive diagnosis of diabetes based on metal–oxide–semiconductor materials

Yujie Li(李育洁)^{1,2}, Min Zhang(张敏)³, and Haiming Zhang(张海明)^{1,†}

¹School of Material Science and Engineering, Tiangong University, Tianjin 300387, China

²Physical Department, Tianjin University Renai College, Tianjin 301636, China

³Department of Obstetrics Tianjin Hospital of ITCWM, Nankai Hospital, Tianjin 300100, China

(Received 2 June 2020; revised manuscript received 5 July 2020; accepted manuscript online 15 July 2020)

In recent years, clinical studies have found that acetone concentration in exhaled breath can be taken as a characteristic marker of diabetes. Metal–oxide–semiconductor (MOS) materials are widely used in acetone gas sensors due to their low cost, high sensitivity, fast response/recovery time, and easy integration. This paper reviews recent progress in acetone sensors based on MOS materials for diabetes diagnosis. The methods of improving the performance of acetone sensor have been explored for comparison, especially in high humidity conditions. We summarize the current excellent methods of preparations of sensors based on MOSs and hope to provide some help for the progress of acetone sensors in the diagnosis of diabetes.

Keywords: non-invasive diabetes diagnosis, acetone sensor, selective, high humidity

PACS: 07.07.Df, 68.35.bg, 73.22.–f, 68.43.–h

DOI: 10.1088/1674-1056/aba60b

1. Introduction

With the development of economy and the improvement of people's living standard, the prevalence of diabetes is increasing year by year in the world. According to the estimation of the World Health Organization (WHO), 693 million diabetics adults will suffer from diabetes worldwide by 2045, compared to 451 million in 2017.^[1] "Prevention is better than cure". Diabetes is a group of metabolic diseases characterized by hyperglycemia. Currently, there is no cure for diabetes but to control blood glucose in some ways. At present, the diagnosis of blood glucose requires multiple traumatic blood tests every day. However, long-term hyperglycemia can lead to serious complications, such as heart attack, kidney failure, stroke, vision loss, leg amputation or nerve damage.^[2] Therefore, it is important to develop a non-invasive, reliable and convenient real-time detection instrument for diabetic patients.

Clinical studies have found that acetone concentration in exhaled breath is more than 1.8 ppm in diabetes and lower than 0.9 ppm in health people.^[3–5] And acetone concentration in exhaled breath is directly related to blood glucose level. Human exhaled breaths are complicated because thousands of volatile organic compounds being contained, which is high in humidity and extremely low in acetone concentrations.^[6,7] The acetone sensors should be sensitive and selective enough to trace acetone concentrations in the exhaled breath down to sub-ppm concentration in high humidity, which is a great challenge to sensors for diabetes diagnosis. Some researchers have tried to reduce the effect of humidity to 20% by pretreating

exhaled breath with molecular sieves.^[8] However, it not only increases the cost of the sensors but also makes them bulky and less portable.

Sensors based on MOSs such as SnO₂, ZnO, WO₃, Co₃O₄, In₂O₃ are considered as the promising sensing materials due to their low cost, high sensitivity, fast response/recovery time, and easy integration in the field of breath biomarkers detection.^[9–13] The mechanism of the MOSs sensor is that the variation of resistance in the air and target gas caused by adsorption/desorption of oxygen species on the sensors.^[14,15] Take the n-type semiconductor sensor as an example. When the sensor is in air, the oxygen molecules are adsorbed onto the surface of the sensor to form O₂⁻, O⁻ or O²⁻, which will reduce the electron concentration from the conduction band and result in increasing of the sensor's resistance. When the sensor encounters a reducing gas, the oxygen ions react with the gas and release electrons back into the conduction band, thus the conductivity of the sensor increased and the resistance of sensor decreased. Thus, the performance of the sensor is mainly determined by the following three: receptor function, transducer function, and utility factor.^[16] First, the receptor function is mainly determined by the amount of oxygen adsorbed on the surface. The larger specific surface area (SSA) provides more opportunities for oxygen adsorption.^[17] Second, the conversion function mainly depends on the surface potential, trapping states in grain boundaries, and defect states in the structure. The results show that the optimization of grain boundary, such as the construction of composite structure, the increase of oxygen vacancy, doping, and noble metal modi-

[†]Corresponding author. E-mail: zhmtjwl@163.com

fication, plays important roles in the enhancement of sensor performances.^[18–21] Third, the utility factor is related to the diffusion and reaction of target gas through structural pores. Porosity of materials is an important parameter to obtain the high utility factor.^[22]

Researchers have done a lot of work to improve the performance of acetone sensors in order to make acetone sensors useful for diagnosing glucose levels of diabetes. However, there are several key issues that have not been resolved simultaneously. The first is the high sensitivity and low limit of detection. A sensor can give effective response when the acetone concentrations are lower than 1.8 ppm, which is the sensitivity that must be achieved for diabetes detection. The second is the selectivity. How to avoid the cross-response of the sensor towards different gases is one of the most critical challenge for gas sensor based on MOSs. The third is the negative effect of humidity. High humidity inhibits the performance of the MOSs' sensor seriously while more than 80% water content is contained in exhaled breath. The fourth one is the effect of working temperature. Most of sensors based on MOSs work 200 °C and 500 °C which will reduce the lifetime of device and increase the power consumption.^[23–26] Apart from the above points, the stability, portability, and response speed are also the issues determining whether the sensor can be commercialized in the field of diabetes diagnosis.^[27]

Professor Han's team enhanced the selectivity by designing an array sensor. But the detection of acetone concentration is down to 5 ppm which is not enough to detect the breath acetone of diabetes.^[28] Zhu *et al.* have presented an acetone sensor based on cobalt-doped ZnO nanoparticles derived from metal–organic frameworks, which enhanced the sensitivity down to 170 ppb and long-term stability for 4 months.^[29] Wang *et al.* have reported an acetone sensor based on porous SnO₂–ZnO hollow microspheres, which exhibited high response to 1.8-ppm acetone under 98% relative humidity.^[30] The sensor could identify the exhaled breath of healthy people and simulated diabetics. However, the diagnosis accuracy and the relationship between sensor response and blood glucose needs further study. This paper reviews recent progress

in acetone sensors based on MOSs for diabetes diagnosis. The performance of the sensor largely depends on the preparation of the sensor materials. Therefore, the methods of enhancing the performance of acetone sensor including morphology improved, noble metal modified, rare earth doping, and composite structures designed are summarized.

2. The methods of enhancing the performance of acetone sensors

2.1. Improving the morphology of MOSs

Different morphologies of structures with specific surface area, exposed surfaces, crystal surface activity, and porosity have a crucial impact on the properties of sensors. Over the past few decades, attempts have been made to increase SSA and magnify the porosity in order to enhance the receptor function and utility factor. Different dimensional structures like 0-dimensional (0D),^[31,32] one-dimensional (1D),^[33,34] two-dimensional (2D),^[35–37] and three-dimensional (3D) structures^[38–41] have been reported for acetone gas sensors. Srinivasan *et al.* reported an acetone sensor using nanostructured Co₃O₄ thin films with the shifting of plane orientation from (311) to (220) at 773 K that showed a sensing response of 235 at room temperature towards 50 ppm and a lower detection limit of 1 ppm of acetone.^[36] It is revealed that the Co₃O₄ thin films deposited at 773 K with rougher surface structure and more reactive oxygen sites resulted in the increased sensing response in-turn. Besides, porous structure had made important applications in the field of gas sensors.^[42–47] Xu *et al.* reported a mesoporous nanofiber made of WO₃ with a crystalline framework with uniform pore size used SnO₂ as hard template to synthesis in an electrospinning method.^[42] It indicated that the fiber-like morphology of WO₃ consists of numerous mesopores, which can offer abundant active sites to interact with guest molecules. Wang *et al.* fabricated a 3D ordered macro/mesoporous (3DOM) C-doped WO₃ sensor and showed that the size of the basic building units plays an important role in acetone responses in 3DOM structure.^[44]

Table 1. The performance of sensors based on MOSs of different sphere structures.

Materials	Morphology	SSA/m ² ·g ⁻¹	Pore/nm	Concentration/ppm	Temperature/°C	Response	(<i>t</i> _{res} / <i>t</i> _{rec})/s	LOD/ppm	Reference
Co ₃ O ₄	porous microspheres	21.2	–	100	180	<i>R</i> _g / <i>R</i> _a = 7.6	2/5	10	[39]
SnO ₂	nanospheres	38.86	22.61	50	220	<i>R</i> _a / <i>R</i> _g = 5.1	8/27	0.246	[46]
SnO ₂	elephantidens-like nanospheres	161.16	3	50	180	<i>R</i> _a / <i>R</i> _g = 37	–	–	[47]
In ₂ O ₃	microspheres	30.3	~ 4 and 80	100	275	<i>R</i> _a / <i>R</i> _g = 13.2	1/51	–	[48]
ZnO	hollow microspheres	42.6	~ 9 and ~ 60	100	350	<i>R</i> _a / <i>R</i> _g = 17.2	1/20	5	[30]
ZnO	double-shelled microspheres	76.11	~ 70	100	300	<i>R</i> _a / <i>R</i> _g = 101.1	1/7	0.5	[43]

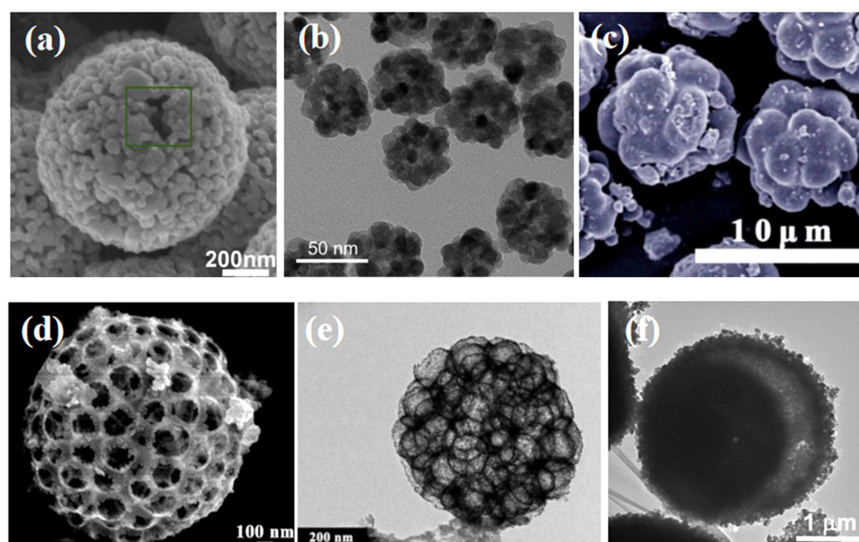


Fig. 1. SEM/TEM images of the materials in Table 1. (a) Co_3O_4 porous microspheres in Ref. [39]; Reproduced with permission from Ref. [39]. (b) SnO_2 nanospheres in Ref. [46]; Reproduced with permission from Ref. [46]. (c) SnO_2 elephantidens-like nanospheres in Ref. [47]; Reproduced with permission from Ref. [47]. (d) In_2O_3 microspheres in Ref. [48]; Reproduced with permission from Ref. [48]. (e) ZnO hollow microspheres in Ref. [30]; Reproduced with permission from Ref. [30]. (f) ZnO double-shelled microspheres in Ref. [43]. Reproduced with permission from Ref. [43].

The sensor based on 3D spherical structure with different SSA and porosity exhibited different acetone sensing performances. Table 1 compares the performance of sensors with different spherical structures in recent years. With the increase of SSA, the response of the sensor to acetone is better. It can be seen from Refs. [46,47] that SnO_2 with a larger SSA reveals a higher response to acetone at a lower operating temperature. Compared to the acetone sensor in Refs. [30,48], the ZnO sensor in Ref. [43] exhibited a higher response and a lower LOD benefiting from the larger SSA and appropriate porosity. Larger SSA provided more active sites for oxygen adsorption, and appropriate porosity promoted gas exchange. Therefore, the performance of sensors depends on the morphologic structure of materials to some extent.

2.2. Noble metal modified

Noble metal is a kind of efficient redox catalyst. The modification of noble metal on the metal–oxide surface can greatly improve the reactivity of the metal–oxide surface. As a catalyst, noble metal modification on the metal–oxide surface can significantly reduce the activation, accelerate the electron transfer rate, provide more specific adsorption sites for oxygen. In addition, the catalytic effect of noble metals is believed that noble metals can decompose hydrocarbons into more ac-

tive free radicals and increase the reaction between oxygen ions and the target gas. Therefore, numbers of noble metals have been used to improve the performance of the acetone sensor for diabetes diagnose,^[49–54] as shown in Table 2.

Liu *et al.* reported three sensors made of Au-, Ag-, Pt-modified In_2O_3 nanowires (NWs) synthesised by electrospinning method^[51] (Fig. 2). It is reported that the modified In_2O_3 NWs can not only heighten the sensing performance, but also effectively enhance the selectivity. The response values of Au-Ag-, Pt-modified NWs sensors were 3.5–4.1 times higher than that of the pristine In_2O_3 NW sensor to 1 ppm of target gases, whereas the detection limits were 4–12.5 times lower than the pristine In_2O_3 NW sensor, as shown in Figs. 2(e)–2(g). A sensing array composed of Au-, Ag-, Pt-modified sensors was made for breath analysis. It demonstrated that the selectivities of gas sensors were greatly improved by the sensing array composed of different noble metal functioned In_2O_3 .

Choi *et al.* fabricated p-type $\text{CuO}/\text{Cu}_2\text{O}$ nanopattern based chemiresistor implied by Ag nanoparticles using a low-energy argon ion bombardment process via a unique top-down lithographic approach.^[53] It was found that the $\text{CuO}/\text{Cu}_2\text{O}/\text{Ag}$ nanopattern presented a performance of 8.04 which was 3.5 times higher than that of the original $\text{CuO}/\text{Cu}_2\text{O}$

Table 2. The performance of sensors based on MOSs functioned by noble metals for acetone detecting.

Materials	Morphology	Concentration/ppm	Humidity/%	Temperature/ $^{\circ}\text{C}$	Response	LOD/ppb	Reference
Ru/WO_3	nanoparticles	1.5	–	300	$R_a/R_g = 7.3$	500	[49]
Pt/SnO_2	3D spheres	5	90	400	$R_a/R_g = 44.8$	200	[50]
$\text{Pt}/\text{In}_2\text{O}_3$	nanowires	1	–	300	$R_a/R_g = 17.9$	20	[51]
Au/ZnO	nanorods	5	–	150	$R_a/R_g = 44.5$	5	[52]
Pt/SnO_2	pill-like network	0.2	80	300	$R_a/R_g = 1.4$	3.6	[7]
$\text{Ag}/\text{CuO}/\text{Cu}_2\text{O}$	nanopattern	0.125	–	300	$\Delta R/R_a = 8.04$	–	[53]
PdAu/SnO_2	3D nanosheets	2	94	250	$R_a/R_g = 6.5$	45	[54]

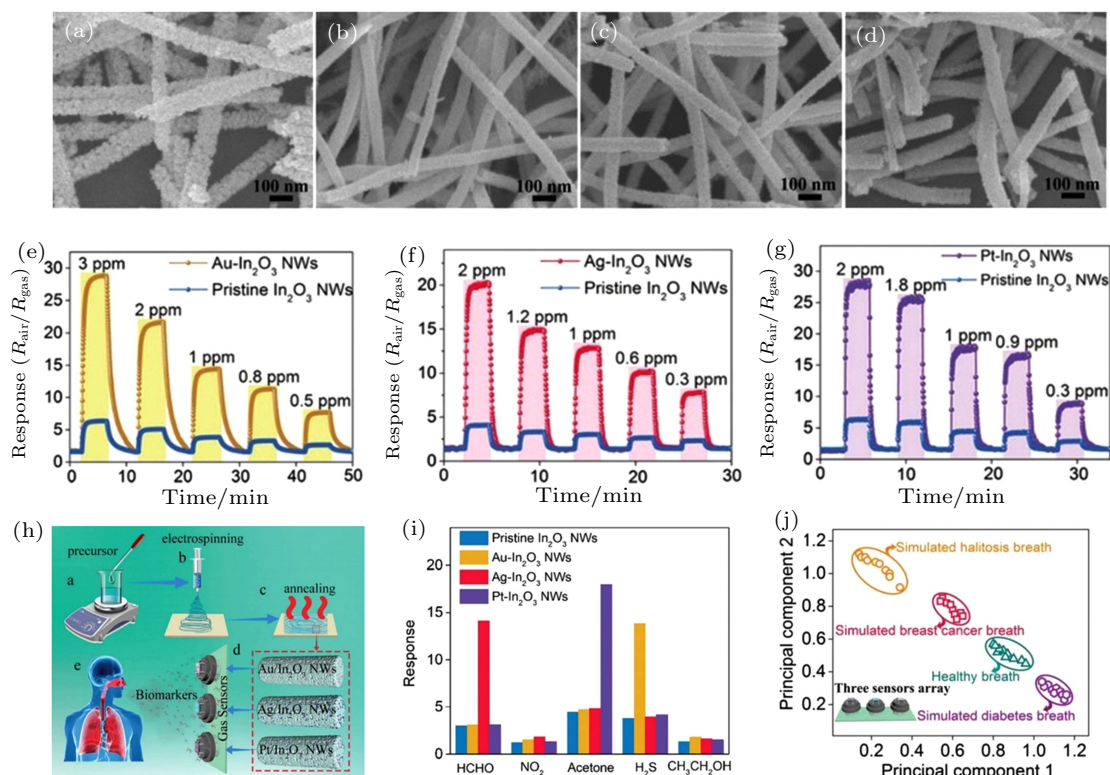


Fig. 2. SEM images of (a) pristine In_2O_3 NWs, (b) $\text{Au-In}_2\text{O}_3$ NWs, (c) $\text{Ag-In}_2\text{O}_3$ NWs, and (d) $\text{Pt-In}_2\text{O}_3$ NWs. Dynamic response curves of (e) $\text{Au-In}_2\text{O}_3$ and pristine In_2O_3 NWs, (f) $\text{Ag-In}_2\text{O}_3$ and pristine In_2O_3 NWs, (g) $\text{Pt-In}_2\text{O}_3$ and pristine In_2O_3 NWs, (h) schematic diagram of the electrospinning process for In_2O_3 NWs and the preparation of the sensor array, (i) selective tests of three gas sensors, (j) pattern recognition based on PCA using three sensor arrays. Reproduced with permission from Ref. [51].

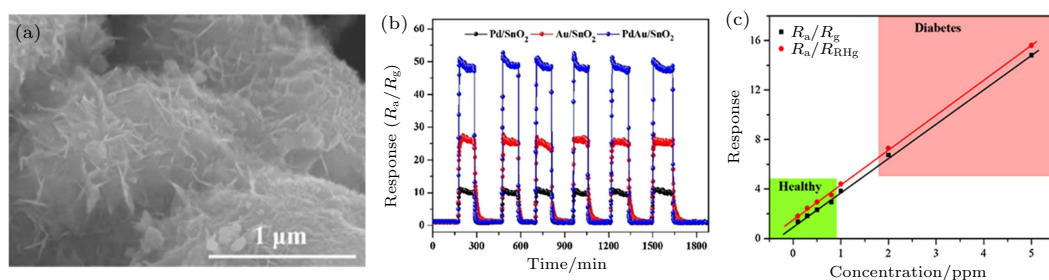


Fig. 3. (a) FESEM image of PdAu/SnO_2 ; (b) six periods of response curve of three sensors to 20-ppm acetone at working time of 250°C ; (c) the response of the PdAu/SnO_2 sensor to different concentrations of acetone in 94% RH environment at working temperature of 250°C . Reproduced with permission from Ref. [54].

nanopattern at the acetone concentration of 0.125 ppm. The effect of the size of the Ag particle was also studied. The $\text{CuO/Cu}_2\text{O/Ag}$ nanopattern with 13-nm Ag exhibited a high gas response, which is 2.7 times higher than that with 31-nm Ag. It demonstrated that the key role of the noble metal modified in improving the performance of acetone sensors based on MOSs.

Acetone sensor research based on bimetallic functional metal oxide was also carried out. Li *et al.* reported that bimetal PdAu decorated SnO_2 nanosheets sensor demonstrated dual selectivity for detecting acetone and formaldehyde at different temperatures,^[54] as shown in Fig. 3. PdAu/SnO_2 had higher performance to acetone than single-metal-modified or pure SnO_2 sensors. Moreover, it was amazing that the response values of PdAu/SnO_2 sensor exhibited the same liner relationship in humidity of 94% environment and in dry air, revealing that the bimetal PdAu -decorated SnO_2 sensor showing excel-

lent acetone response at high humidity.

2.3. Rare earth doping

Rare earth elements like La-, Ce-, Yb-, Pr-, Tb-, Ho-, Nd-doped MOSs are widely used in the preparation of acetone sensor because of their excellent catalytic properties, also serve as sensitizers which greatly increases the active sites on the surface of metal oxides. A method of La-doped ZnO with unique bead-like structures was reported.^[23] The gas sensing results showed that 1.0-wt% La-doped ZnO nanofibers improved the response to acetone significantly. Yang *et al.* reported La_2O_3 -doped Zn_2SnO_4 hollow fibers by electrospinning investigated for acetone detection.^[55] Compared with Zn_2SnO_4 fibers, the La_2O_3 -doped Zn_2SnO_4 hollow fibers not only enhanced sensing sensitivity, but also reduced the working temperature from 240°C to 200°C . Ying *et al.* prepared Ce-doped NdVO_4 nanorods by a facile one-step hydrother-

mal method.^[56] The study showed that with the increase of Ce doping concentration, the semiconductor properties to $Ce_xNd_{1-x}VO_4$ changed from n-type to p-type and then to n-type. The appropriate doping concentration had an optimal response to acetone at low working temperature of 108 °C. In another work, 0.5-wt% La-doped SnO_2 exhibited a response of 3626 toward 400-ppm acetone at 350 °C.^[57]

Reducing the effect of high humidity on the performance of sensor based on MOSs must be considered in the detection of acetone concentrations in the exhaled breath which is still a huge challenge. Unlike additives with high affinity for water,^[7,50,54] Lee's team reported Ce-doped In_2O_3 , Tb-doped SnO_2 , and Pr-doped In_2O_3 significantly suppressed the degradation of gas-sensing characteristics by mitigating water-poisoning effect due to tri/tetravalent states, as shown in Fig. 4.

The 11.7-wt% Ce- In_2O_3 sensor had a response of ≈ 0.9 of the S_{wet}/S_{dry} as well as a low detection limit (500 ppb) and excellent acetone selectivity even in humidity of 80% which exhibited humidity-independent gas sensing characteristics.^[58] Terbium-doped SnO_2 yolk-shell spheres sensor showed a high response of 1.21 to 50 ppb of acetone in 80% humidity with low responses to the other interference gases.^[59] The 12-at.% Pr-doped In_2O_3 macroporous spheres sensor exhibited the detection limitation concentration was 85 ppb when $R_a/R_g > 1.2$ and showed excellent selectivity values to acetone under the humidity of 80%.^[60] The studies revealed that the coexistence of tri/tetravalent states such as Ce^{3+}/Ce^{4+} , Te^{3+}/Te^{4+} , and Pr^{3+}/Pr^{4+} prevents the water-poisoning effect by removing the hydroxyl group and regenerating the oxygen adsorption.

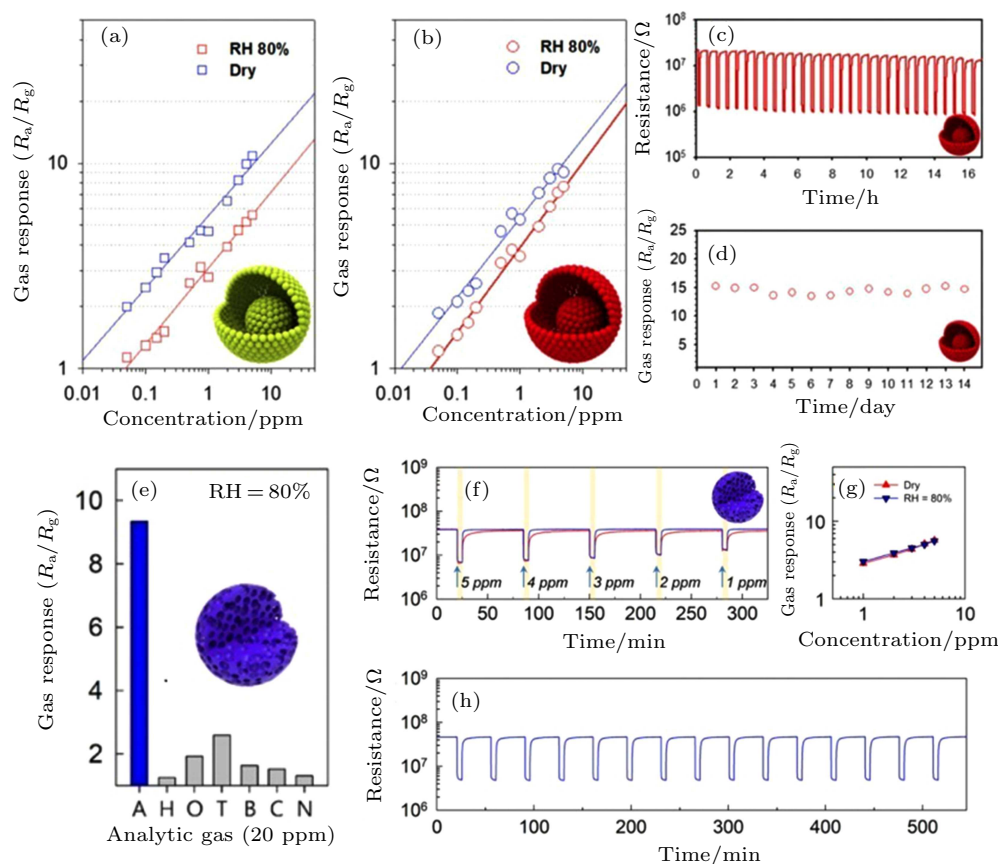


Fig. 4. Gas responses of the (a) pure SnO_2 and (b) 5Tb- SnO_2 sensors to acetone at 450 °C under both humid and dry conditions; (c) 30 repetitive sensing transients to 20-ppm acetone and (d) long-term stability of 5Tb- SnO_2 sensor at 450 °C in RH 80%. Reproduced with permission from Ref. [59]. (e) Gas responses of the 12Pr- In_2O_3 macroporous spheres to 20 ppm of acetone. (f) Dynamic sensing transients, (g) responses and (h) 15 repetitive sensing transients of the 12Pr- In_2O_3 macroporous spheres to 20-ppm acetone at 450 °C. Reproduced with permission from Ref. [60].

2.4. Designing composite structures

It is reported that the performance of acetone sensor can be enhanced by improving the material structure. However, there are some problems that have not been solved such as low sensitivity, poor selectivity, and high working temperature. Recently, n-n, p-n heterostructure composites, and graphene/MOSs composites have attracted significant attention as functional materials due to the higher sensitivity and

faster response.^[30,61–67]

Wang *et al.* fabricated 3D opal porous SnO_2 -ZnO hollow microspheres by employing sulfonated polystyrene spheres template-assisted ultrasonic spray pyrolysis (Fig. 5).^[30] The 3D SnO_2 -ZnO sensor exhibited high response and ultra-fast dynamic process (response time ~ 4 s and recovery time ~ 17 s) to 1.8-ppm acetone especially under 98% relative humidity. Porous structures and p-n heterostructures played important roles in improving gas sensitivity in high humidity.

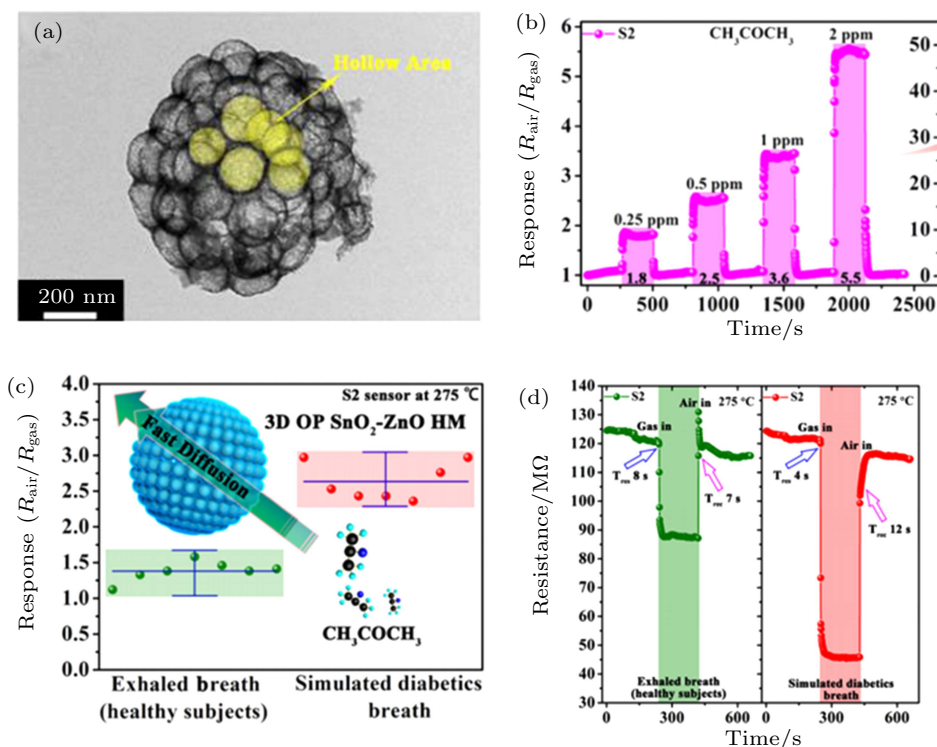


Fig. 5. (a) TEM images of 3D OP SnO₂-ZnO HM; (b) the sensor-based SnO₂-ZnO HM to acetone in the range 0.25 ppm–100 ppm at 275 °C; (c) the identification of human exhaled breath (healthy subjects and simulated diabetics) based on SnO₂-ZnO sensor; (d) dynamic resistance change transients of the SnO₂-ZnO sensor to human exhaled breath. Reproduced with permission from Ref. [30].

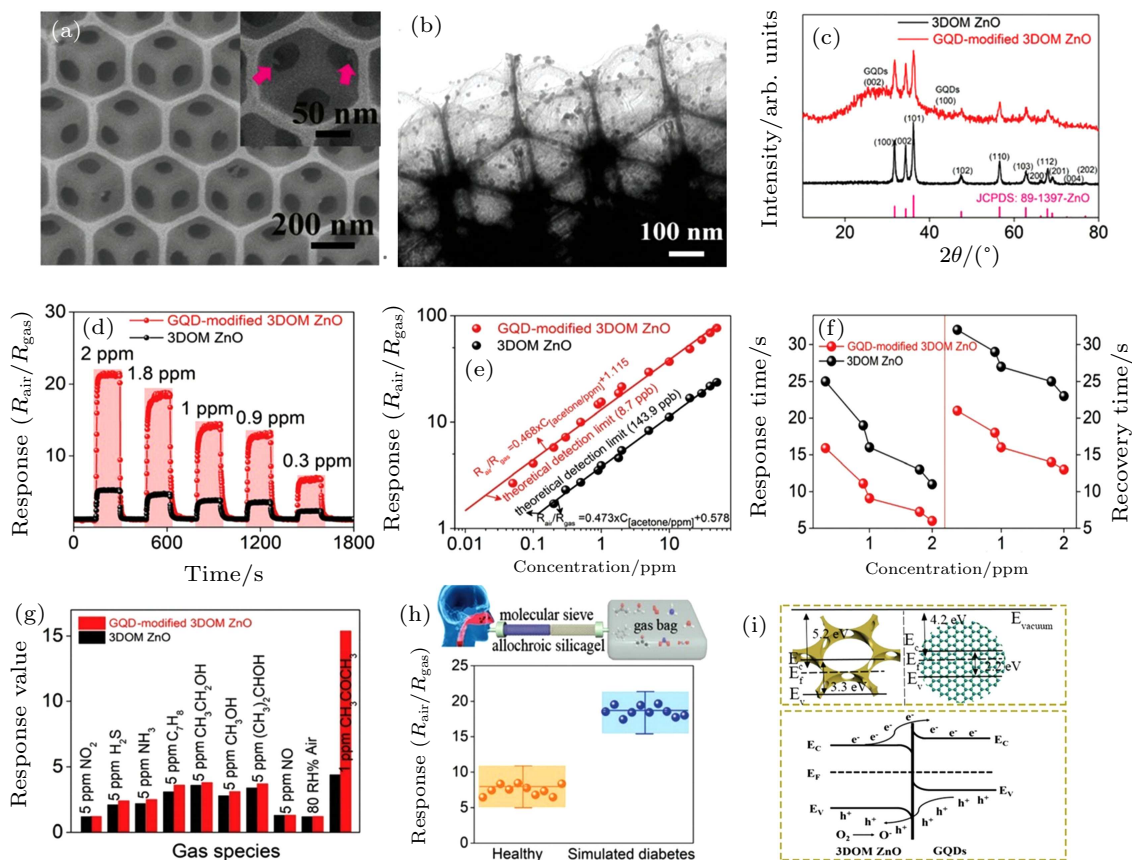


Fig. 6. (a) The SEM and (b) TEM images of the GQD-modified 3DOM ZnO sample; (c) XRD patterns of 3DOM ZnO and GQD-modified 3DOM ZnO samples; (d) the dynamic response curves in the acetone concentration range of 0.3 ppm–2 ppm; (e) the linear relationship response of various acetone concentrations; (f) the response/recovery time to acetone; (g) the selectivity tests for the 3DOM ZnO sensor and GQD-modified 3DOM ZnO sensor; (h) the responses of the GQD-modified 3DOM ZnO sensor toward healthy and simulated diabetes exhaled breaths and a schematic diagram of the breath collecting process; (i) the band diagram structure. Reproduced with permission from Ref. [8].

Xue *et al.* reported the preparation of ZnO@MoS₂ core-shell heterostructures.^[61] The response of sensor based on ZnO@MoS₂ nanostructures was 80 times higher than that of the pure ZnO to acetone, and the LODs reached to 5 ppb. It showed that the metal-oxide composite can effectively improve the sensitivity of the gas sensor.

Graphene/MOSs and carbon/MOSs composites has aroused greatly attention due to their sufficient conductivity and the formation of p-n junction which has achieved significant applications for diabetes diagnosis.^[8,68-74] Liu *et al.* reported a kind of graphene quantum dot (GQDs) functionalized 3DOM ZnO for acetone detection,^[8] as shown in Fig. 6. The proposed sensor exhibited R_a/R_g of 15.2 for 1-ppm acetone, response/recovery time of 9 s/16 s, low detection limit down to 8.7 ppb, and good selectivity. Moreover, the GQDs functionalized 3DOM ZnO sensor exhibited a response of at least 3.2 times differences in the health breath from the diabetes breath. The excellent sensing performance may be attributed to the formation of p-n heterojunctions and the large SSA of 88.2 m²·g⁻¹ modified by GODs. In particular, more oxygen vacancy existed in the composite surface due to GQD-modified effect. The processes led to a change in the electron concentration in the conductive layer.

3. Conclusions and outlook

Non-invasive detection of diabetes by analyzing human breath is a rapid, low-cost, and simple blood analysis method. Sensors based on MOSs have attracted wide attention in recent years due to their advantages of high sensitivity, simple fabrication, and ease of integration. In the face of many challenges such as sensor selectivity, high humidity, slow response, and high working temperature, different methods including morphology improved, noble metal modified, rare earth doping, and composite structures designed have been explored for sensors based on MOSs. The appropriate sensitivity, detection limit, and selectivity at high humidity are still the key points to be overcome in the detection of diabetes' exhaled breath. However, the mechanism of the acetone sensor should be further studied in order to accelerate the process of improving the performance of the sensor.

In order to overcome the challenges, the future breath acetone sensor should focus on (i) significant achievement with high sensitivity at low concentrations specific to acetone operated at room temperature; (ii) long-term stable and accurate diagnosis of diabetes on the sensor technologies; (iii) the background level of the interfering compounds and the variations in the breath cycle; (iv) real-time dynamic intelligent identification system development.

References

[1] Shokrehodaie M and Quinones S 2020 *Sensors* **20** 1251

- [2] Usman F, Dennis J O, Ahmed A Y, Meriaudeau F, Ayodele O B and Rabih A A S 2019 *IEEE Access* **7** 5963
- [3] Saasa V, Beukes M, Lemmer Y and Mwakikunga B 2019 *Diagnostics* **9** 224
- [4] Konvalina G and Haick H 2014 *Acc. Chem. Res.* **47** 66
- [5] Afreen S and Zhu J J 2019 *Trends Anal. Chem.* **118** 477
- [6] Rydosz A 2018 *Sensors* **18** 2298
- [7] Moon H G, Jung Y, Jun D, Park J H, Chang Y W, Park H H, Kang C Y, Kim C and Kaner R B 2018 *ACS Sens.* **3** 661
- [8] Liu W, Zhou X Y, Xu L, Zhu S D, Yang S, Chen X F, Dong B, Bai X, Lu G Y and Song H W 2019 *Nanoscale* **11** 11496
- [9] Zhang J N, Zhang L Z, Leng D Y, Ma F, Zhang Z Y, Zhang Y Y, Wang W, Liang Q F, Gao J Z and Lu H B 2020 *Sens. & Actuators B: Chem.* **306** 127575
- [10] Postica V, Vahl A, Santos C D, Dankwort T, Kienle L, Hoppe M, Cadi E A, de Leeuw N H, Terasa M I, Adelung R, Faupel F and Lupan O 2019 *ACS Appl. Mater. Interfaces* **11** 31452
- [11] Li F, Ruan S P, Zhang N, Yin Y Y, Guo S J, Chen Y, Zhang H F and Li C N 2018 *Sens. Actuators B* **265** 355
- [12] Zhang R, Gao S, Zhou T T, Tu J C and Zhang T 2020 *Appl. Surf. Sci.* **503** 144167
- [13] Liu W, Xie Y L, Chen T X, Lu Q X, Rehman S U and Zhu L 2019 *Sens. & Actuators B: Chem.* **298** 126871
- [14] Mohammad K, Sahar K, Mojtaba A and Alimorad R 2019 *Sens. Actuators B: Chem.* **281** 96
- [15] Li Y J, Zhang H M, Zhang X H, Wei L J, Zhang Y, Hai G Y and Sun Y X 2019 *J. Mater. Sci.: Mater. Electron.* **30** 15734
- [16] Nasiri N and Clarke C 2019 *Sensors* **19** 462
- [17] Kim S J, Choi S J, Jang J S, Cho H J and Kima I D 2017 *Acc. Chem. Res.* **50** 1587
- [18] Kim K H, Kim S J, Cho H J, Kim N H, Jang J S, Choi S J and Kim I D 2017 *Sens. Actuators B* **241** 1276
- [19] Yuan H Y, Aljneibi S A A A, Yuan J R, Wang Y X, Liu H, Fang J, Tang C H, Yan X H, Cai H, Gu Y D, Pennycook S J, Tao J F and Zhao D 2019 *Adv. Mater.* **31** 1807161
- [20] Wang J C, Shi W N, Sun X Q, Wu F Y, Li Y and Hou Y X 2020 *Nanomaterials* **10** 398
- [21] Cui W, Kang X L, Zhang X Y, Zheng Z and Cui X D 2019 *Physica E: Low-dimensional Syst. Nanostruct.* **113** 165
- [22] Lu Y Y, Zhan W W, He Y, Wang Y T, Kong X J, Kuang Q, Xie Z X and Zheng L S 2014 *ACS Appl. Mater. Interfaces* **6** 4186
- [23] Xu X L, Chen Y, Ma S Y, Li W Q and Mao Y Z 2015 *Sens. Actuators B* **213** 222
- [24] Deepapriya S, Devi S L, Vinosha P A, Rodney J D, Raj C J, Jose J E and Das S J 2019 *Appl. Phys. A* **125** 683
- [25] Qin Y X, Liu C Y and Liu Y 2015 *Chin. Phys. B* **24** 027304
- [26] Li Y Z, Feng Q J, Shi B, Gao C, Wang D Y and Liang H W 2020 *Chin. Phys. B* **29** 018102
- [27] Liu T, Li L Y, Yang X Y, Liang X S, Liu F M, Liu F M, Zhang C, Sun P, Yan X and Lu G Y 2019 *Sens. & Actuators B: Chem.* **296** 126688
- [28] Song L F, Yang L P, Wang Z, Liu D, Luo L Q, Zhu X X, Xi Y, Yang Z X, Han N, Wang F Y and Chen Y F 2019 *Sens. & Actuators B: Chem.* **283** 793
- [29] Zhu S D, Xu L, Yang S, Yang S, Zhou X Y, Chen X F, Dong B, Bai X, Lu Z Y and Song H W 2020 *J. Colloid Interface Science* **569** 358
- [30] Wang T S, Zhang S F, Yu Q, Wang S P, Sun P, Lu H Y, Liu F M, Yan X and Lu G Y 2018 *ACS Appl. Mater. Interfaces* **10** 32913
- [31] Yoo R, Park Y J, Jung H, Rim H J, Cho S, Lee H S and Lee W 2019 *J. Alloys Compd.* **803** 135
- [32] Wang X, Xia R, Jiang S B, Gao M Z and Bao H F 2020 *Appl. Surf. Sci.* **507** 145094
- [33] Zhang W S, Fan Y, Yuan T W, Lu B, Liu Y M, Li Z X, Li G J, Cheng Z X and Xu J Q 2020 *Adv. Mater. Interfaces* **12** 3755
- [34] Tomi M, Šetka M, Chmela O, Gracia I, Figueras E, Cane C and Vallejos S 2018 *Biosensors* **8** 116
- [35] Ge W Y, Jiao S Y, Chang Z, He X M and Li Y X 2020 *ACS Appl. Mater. Interfaces* **12** 13200
- [36] Srinivasan P, Kulandaisamy A J, Mani G K, Babu K J, Tsuchiya K and Rayappan J B B 2019 *RSC Adv.* **9** 30226
- [37] Ding H, Ma J L, Yue F, Gao P Y and Jia X 2019 *J. Solid State Chem.* **276** 30
- [38] Zhang D, Fan Y, Li G J, Du W, Li R L, Liu Y M, Cheng Z X and Xu J Q 2020 *Sens. & Actuators B: Chem.* **302** 127187

- [39] Cao J, Wang S M, Zhang H M and Zhang T 2019 *Mater. Sci. Semicond. Process.* **101** 10
- [40] Zou Y D, Zhou X R, Zhu Y H, Cheng X W, Zhao D Y and Deng Y H 2019 *Acc. Chem. Res.* **52** 714
- [41] Zhang R, Shi J W, Zhou T T, Tu J C and Zhang T 2019 *J. Colloid Interface Sci.* **539** 490
- [42] Xu H Y, Gao J, Li M H, Zhao Y Y, Zhang M, Zhao T, Wang L J, Jiang W, Zhu G J, Qian X Y, Fan Y C, Yang J P and Luo W 2019 *Front. Chem.* **7** 266
- [43] Li Y J, Wang S M, Hao P, Tian J, Cui H Z and Wang X Z 2018 *Sens. & Actuators B: Chem.* **273** 751
- [44] Wang M D, Li Y Y, Yao B H, Zhai K H, Li Z J and Yao H C 2019 *Sens. & Actuators B: Chem.* **288** 656
- [45] Li Y H, Zhou X R, Luo W, Cheng X W, Zhu Y H, El-Toni A M, Khan A, Deng Y H and Zhao D Y 2019 *Adv. Mater. Interfaces* **6** 1801269
- [46] Hu J, Yang J, Wang W D, Xue Y, Sun Y J, Li P W, Lian K, Zhang W D, Chen L, Shi J and Chen Y 2018 *Mater. Res. Bull.* **102** 294
- [47] Lian X X, Li Y, Zhu J W, Zou Y L, Liu X L, An D M and Wang Q 2019 *Curr. Appl. Phys.* **19** 849
- [48] Wang T S, Can I, Zhang S F, He J M, Sun P, Liu F M and Lu G Y 2018 *ACS Appl. Mater. Interfaces* **10** 5835
- [49] Li Y, Hua Z Q, Wu Y, Zeng Y, Qiu Z L, Tian X M, Wang M J and Li E P 2018 *Sens. & Actuators B: Chem.* **265** 249
- [50] Cho H J, Choi S J, Kim N H and Kim I D 2020 *Sens. & Actuators B: Chem.* **304** 127350
- [51] Liu W, Sun J, Xu L, Zhu S D, Zhou X Y, Yang S, Dong B, Bai X, Lu G Y and Song H W 2019 *Nanoscale Horiz.* **4** 1361
- [52] Huang J Y, Zhou J X, Liu Z H, Li X J, Geng Y F, Tian X Q, Du Y and Qian Z F 2020 *Sens. & Actuators B: Chem.* **310** 127129
- [53] Choi Y M, Cho S Y, Jang D Y, Koh H J, Choi J, Kim C H and Jung H T 2019 *Adv. Funct. Mater.* **29** 1808319
- [54] Li G J, Cheng Z X, Xiang Q, Yan L M, Wang X H and Xu J Q 2019 *Sens. & Actuators B: Chem.* **283** 590
- [55] Yang H M, Ma S Y, Yang G J, Chen Q, Zeng Q Z, Ge Q, Ma L and Tie Y 2017 *Appl. Surf. Sci.* **425** 585
- [56] Ying M H, Hou J M, Xie W Q, Xu Y J, Shen S F, Pan H B and Du M 2018 *Sens. & Actuators B: Chem.* **260** 125
- [57] Tammanoon N, Wisitsoraat A, Phokharatkul D, Tuantranont A, Phanichphant S, Yordsri V and Liewhiran C 2018 *Sens. & Actuators B: Chem.* **262** 245
- [58] Yoon J W, Kim J S, Kim T Y, Hong Y J, Kang Y C and Lee J H 2016 *Small* **12** 4229
- [59] Kwak C H, Kim T H, Jeong S Y, Yoon J W, Kim J S and Lee J H 2018 *ACS Appl. Mater. Interfaces* **10** 18886
- [60] Kim J S, Na C W, Kwak C H, Li H Y, Yoon J W, Kim J H, Jeong S Y and Lee J H 2019 *ACS Appl. Mater. Interfaces* **11** 25322
- [61] Xu Y S, Zheng L L, Yang C, Liu X H and Zhang J 2020 *Sens. & Actuators B: Chem.* **304** 127237
- [62] Cao E, Song G Q, Guo Z Q, Zhang Y J, Hao W T, Sun L and Nie Z Q 2020 *Mater. Lett.* **261** 126985
- [63] Shao H Y, Huang M X, Fu H, Wang S P, Wang L W, Lu J, Wang Y H and Yu K F 2019 *Front. Chem.* **7** 785
- [64] Rahman M, Alam M M, Asiri A M and Islam M A 2017 *Talanta* **170** 215
- [65] Poovaragan S, Sundaram R, Magdalane C M, Kaviyarasu K and Maaza M 2019 *J. Nanosci. Nanotechnol.* **19** 859
- [66] Shao S F, Chen X, Chen Y Y, Lai M and Che L S 2019 *Appl. Surf. Sci.* **473** 902
- [67] Zhang J N, Lu H, Lu H B, Li G, Gao J Z, Yang Z B, Tian Y H, Zhang M, Wang C L and He Z 2019 *J. Alloys Compd.* **779** 531
- [68] Liu L, Zhang D M, Zhang Q, Chen X, Xu G, Lu Y L and Liu Q J 2017 *Biosensors and Bioelectronics* **93** 94
- [69] Liu C, Zhao L P, Wang B Q, Sun P, Wang Q J, Gao Y, Liang X S, Zhang T and Lu G Y 2017 *J. Colloid Interface Sci.* **495** 207
- [70] Chu X F, Liu J S, Liang S M, Bai L S, Dong Y P and Epifani M 2019 *J. Sens.* **2019** 6074046
- [71] Zhang D Z, Wu Z L and Zong X Q 2019 *Sens. & Actuators B: Chem.* **288** 232
- [72] Wu K D, Luo Y F, Li Y and Zhang C 2019 *Beilstein J. Nanotechnol* **10** 2516
- [73] Xiong Y, Chang X, Qiao X R, Li K, Zhu L, Xia F J, Li X F, Zheng Q B, Xing W and Xue Q Z 2019 *Sens. & Actuators B: Chem.* **300** 127011
- [74] Jia X H, Cheng C D, Yu S W, Yang J, Li Y and Song H J 2019 *Sens. & Actuators B: Chem.* **300** 127012